

Section AIR POLLUTION AND CLIMATE CHANGE

ANALYSES OF GEOMAGNETIC DATA SETS FROM OBSERVATORIES AND CORRELATION BETWEEN THEM

Dr. Laurențiu Asimopolos¹

Dr. Natalia-Silvia Asimopolos²

Asist. Prof. Adrian-Aristide Asimopolos³

^{1, 2} Geological Institute of Romania, Romania

³ University POLITEHNICA of Bucharest, Romania

ABSTRACT

The purpose of this study was to analyze the associated spectrum of geomagnetic field, frequencies intensity and the time of occurrence. We calculated the variation of the correlation coefficients, with mobile windows of various sizes, for the recorded magnetic components at different latitudes and longitudes.

We included in our study the observatories: Surlari (USA), Honolulu (HON), Scott Base (SBA), Kakioka (KAK), Tihany (THY), Uppsala (UPS), Wingst (WNG) and Yellowknife (YKC). We used the data of these observatories from INTERMAGNET for the biggest geomagnetic storm from the last two Solar Cycles.

We have used for this purpose a series of filtering algorithms, spectral analysis and wavelet with different mother functions at different levels.

In the paper, we show the Fourier and wavelet analysis of geomagnetic data recorded at different observatories regarding geomagnetic storms. Fourier analysis highlights predominant frequencies of magnetic field components. Wavelet analysis provides information about the frequency ranges of magnetic fields, which contain long time intervals for medium frequency information and short time intervals for highlight frequencies, details of the analyzed signals. Also, the wavelet analysis allows us to decompose geomagnetic signals in different waves. The analyzes presented are significant for the studied of the geomagnetic storm. The data for the next days after the storm showed a mitigation of the perturbations and a transition to a quiet day of the geomagnetic field.

In both, the Fourier Transformation and the Wavelet Transformation, transformation evaluation involves the calculation of a scalar product between the analyzed signal and a set of signals that form a particular base in the vector space of the finite energy signals. Fourier representation use an orthogonal vectors base, whereas in the case of wavelet there is the possibility to use also bases consisting of independent linear non-orthogonal vectors. Unlike the Fourier transform, which depends only on a single parameter, wavelet transform type depends on two parameters, a and b. As a result, the graphical representation of the spectrum is different, wavelet analysis bringing more information about geomagnetic pattern of each observatory with that own specific conditions.

Keywords: geomagnetic storm, spectral analysis, Fourier transform, wavelet analysis

INTRODUCTION

Space weather is a main natural threat to critical infrastructures and their security.

Dynamic conditions on the Sun, in the solar wind, and in the near-Earth space environment can influence the performance of man-made technology, and can also affect human health and activities.

In this paper, we present the results obtained for the geomagnetic data acquired at the Surlari Observatory, located about 30 Km North of Bucharest - Romania. The observatory database contains records from the last seven solar cycles, with different sampling rates.

Also, we used data from other observatories [3], from INTERMAGNET geomagnetic network (www.intermagnet.org), <http://www.noaa.gov> and <https://www.spaceweatherlive.com/en/archive>. The aim of the paper is to analyze the series of geomagnetic data recorded at several observatories during major geomagnetic disturbances. In this study, we analyze the data recorded during the strongest storm in the Solar Cycle, 23 from October, 28-31, 2003.

Geomagnetically induced currents (GICs), a space weather-driven phenomenon, have received the increased international policy, science, industry, and public interest.

GICs flowing on ground-based electrically conducting systems can disrupt the operation of critical infrastructure such as power grids, pipelines, telecommunication cables and railway systems [8], [9], as in figure 1.

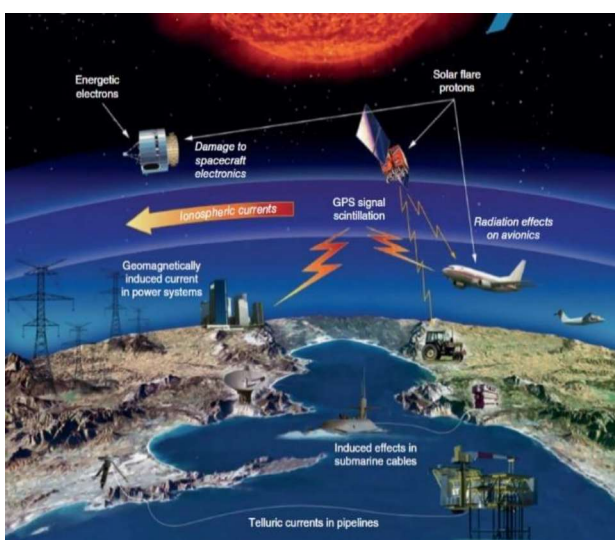


*Fig 1 - Technological infrastructure affected by space weather events at the Earth.
Source: Courtesy of NASA:
<https://www.nasa.gov>.*

A big geomagnetic storm, called the "Halloween Storms of 2003," began after two-three years from solar maximum, when outbreaks 17 major flares (CME), erupted on the Sun. This storm led to a very large

increase in GICs, which caused great damage in the power networks from the countries situated at high northern latitudes.

Section AIR POLLUTION AND CLIMATE CHANGE

METHODOLOGY

For the study of correlations between two geomagnetic time series recorded at two observatories during of geomagnetic storm we used correlation coefficient, in mobile windows.

Pearson correlation coefficient $r_{z/w}$ of two parameters (time series) is:

$$r_{\frac{z}{w}} = \frac{n \sum_{i=1}^n z_i w_i - (\sum_{i=1}^n z_i)(\sum_{i=1}^n w_i)}{\sqrt{[n \sum_{i=1}^n z_i^2 - (\sum_{i=1}^n z_i)^2] \cdot [n \sum_{i=1}^n w_i^2 - (\sum_{i=1}^n w_i)^2]}}$$

where: z_i, w_i are time series of two parameters, n is size of time series.

Multiresolution analysis, through wavelets methodology, allow local analysis of magnetic field components through variable frequency windows. Windows that contain longer time intervals allow us to extract low-frequency information, average ranges of different sizes lead to extraction of medium frequency information, and very narrow windows highlight the high frequencies or details of the analyzed signals. The wavelet functions describe the orthogonal bases in the $L_2(R)$ space, with signal approximation properties, while the orthonormal bases in the Fourier analysis are made up of sinusoidal waves. Estimation of geomagnetic field disturbances is similar to the standard problem of estimating a signal disturbed by signal theory. The term noise refers to any modification that changes the periodic or quasi-periodic characteristics of the original signal. The model of the disturbed geomagnetic field is composed of periodic oscillations plus non-periodic oscillations given by the impact of solar wind on the terrestrial magnetosphere [1], [2].

The purpose of wavelet analysis is to build orthonormal bases composed of wavelets that can reconstruct the geomagnetic signals recorded in the observatories.

The wavelet algorithm was originally formulated by Goupillaud, Grossmann and Morlet in 1984 as a constant κ_σ subtracted from a plane wave and then localized by a Gaussian window [6], [14]:

$$\Psi_\sigma(t) = C_\sigma \pi^{-\frac{1}{4}} e^{-\frac{1}{2} t^2} (e^{i\sigma} - k_\sigma), \text{ where: } k_\sigma = e^{-\frac{1}{2}\sigma^2} \text{ is defined by the admissibility criterion and the normalization constant } C_\sigma \text{ is:}$$

$$C_\sigma = (e^{-\sigma^2} - 2e^{-\frac{3\sigma^2}{4}})^{-\frac{1}{2}}$$

Multiple resolution analysis is the core of wavelet analysis. This involves the decomposition of a signal in the subscripts at different levels of resolution.

The wavelet analysis is based on the decomposition of an approximate, constant portion, of a function f from the space $L_2(R)$ in a rough approximation and a detail function.

At each level j , approximate f_j of the given function f , can be written as a sum of a coarse approximation f_{j-1} located at the next approximation level and the detail



function g_{j-1} , i.e. $f_j = f_{j-1} + g_{j-1}$. Each detail function can be written as a linear combination of mother wavelet functions:

$\psi_{j,k}(x) = 2^{\frac{j}{2}}\psi(2^jx - k)$, where j is the index of dilatation and k is the index of translation, $j, k \in \mathbb{Z}$. When the index j gets higher, the approximate approximations become finer. For each level of resolution, we have a base function space $(\psi_{j,k})$, $j, k \in \mathbb{Z}$. Therefore, we will work with multiple spaces at different resolutions (multiresolution).

The wavelet function is designed to strike a balance between time domain (finite length) and frequency domain (finite bandwidth). As we dilate and translate the mother wavelet, we can see very low frequency components at large s while very high frequency component can be located precisely at small s .

The transition from STFT to wavelet was done by replacing a fixed-length analysis window, regardless of the frequency of the studied signal, with a set of variable duration analysis windows, so that at low frequencies we use long duration, and at high frequencies we use small durations. To make Wavelet Continue Transform (CWT), a real or complex signal must satisfy the following two conditions:

$$\int_{-\infty}^{\infty} \psi(t) dt = 0 \quad , \quad \int_{-\infty}^{\infty} |\psi(t)|^2 dt < \infty$$

The first property, according to which the signal has a mean null value, suggests a possible oscillating aspect, while the second property, referring to the finite energy value, indicates that the signal concentrates most of the energy within a finite range of time.

The two conditions, together with a so-called admissibility condition (required to define the transformed wavelet inverse) are sufficient for a signal to "qualify" as a wavelet signal. In the literature, numerous such signals have been proposed, some of them with finite (thus compact support) and others with infinite duration, but with concentrated energy within a finite timeframe.

In both, the Fourier Transform and the Wavelet Transformation, transformation evaluation involves the calculation of a scalar product between the analyzed signal and a set of signals that form a particular base in the vector space of the finite energy signals. Fourier representation use a orthogonal vectors basis, whereas in the case of wavelet there is the possibility to use also bases consisting of independent linear non-orthogonal vectors. Unlike the Fourier transform, which depends only on a single parameter, wavelet transform type depends on 2 parameters, a and b .

In the wavelet charts, the frequencies are marked with colors between blue and yellow representing the weight of each frequency in the analyzed signal. According to this, we can find the predominant frequency for each component at each time. The STFT tries to solve the problem in Fourier transform by introducing a sliding window $w(t-u)$. The detailed windows are designed to extract a small portion of the signal $f(t)$ and then take Fourier transform. The transformed coefficient has two independent parameters. The wavelet functions are designed to strike a balance between time domain (finite length) and frequency domain (finite bandwidth). As

Section AIR POLLUTION AND CLIMATE CHANGE

we dilate and translate the mother wavelet, we can see very low-frequency components at large scale, while very high-frequency component can be located precisely at a small scale. Another methods used for analyzing of geomagnetic field and prior forecast of geomagnetic storms is Auto-Regressive Integrated Moving Average (ARIMA).

ARIMA models are the most general class of models for forecasting a time series which can be made to be “stationary” by differencing in conjunction with nonlinear transformations. A random time series is stationary if its statistical properties are all constant over time. A stationary series has no trend, its variations around its mean have a constant amplitude, and its short-term random time patterns always look the same in a statistical sense. This condition means that its autocorrelations (correlations with its own prior deviations from the mean) remain constant over time, or equivalently, that its power spectrum remains constant over time [4], [5], [7], [10]. A random variable of this form can be viewed as a combination of signal and noise, and the signal could be a pattern of fast or slow mean reversion, or sinusoidal oscillation, or rapid alternation in sign, and it could also have a seasonal component.

An ARIMA model can be viewed as a “filter” that tries to separate the signal from the noise, and the signal is then extrapolated into the future to obtain forecasts [4], [12].

RESULTS

In figure 2 are shows the North geomagnetic field in October 28, 2003 at Surlari Observatory and spectral analysis. Also, in figure 3, for derived of North geomagnetic field.

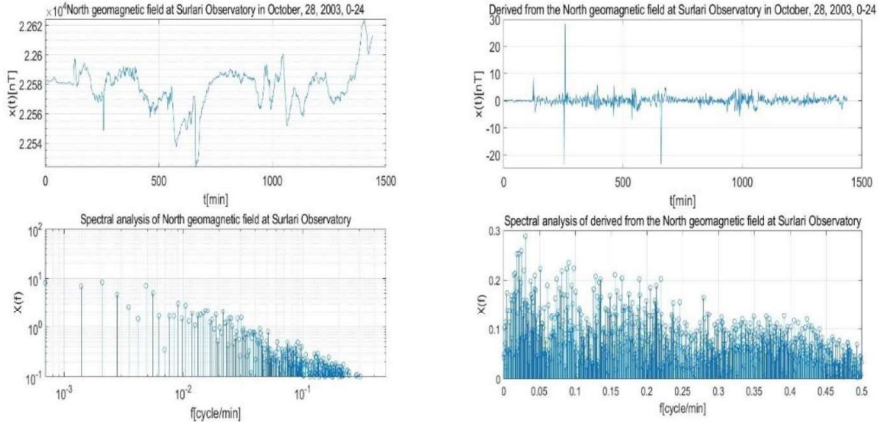


Fig.2-North geomagnetic field on Surlari Observatory, in October 28th, 2003, 0:24, minute mean, and spectral analyses

Fig.3-Derived from the North geomagnetic field on Surlari Observatory, in October 28th, 2003 and spectral analyses



Figures 4-9 shows the wavelet power spectra themselves, an important advantage of wavelet analysis over spectral analysis. On the horizontal axis we have the time dimension. The vertical axis gives us the periods. The power is given by the color. The color code indicates ranges of power from blue to yellow.

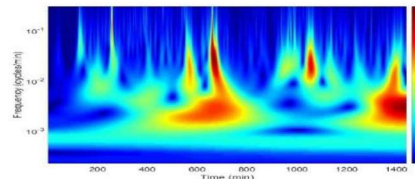
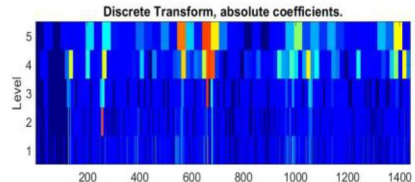


Fig.4 – Absolute coefficients, function db1, level 5 and wavelet image with frequency, time and amplitude, for North geomagnetic field

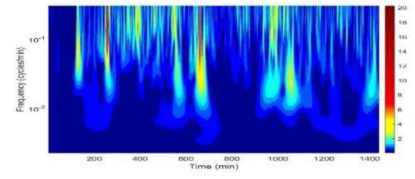
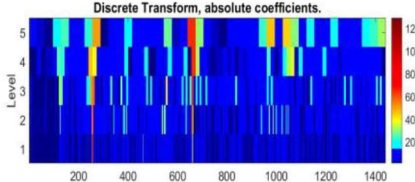


Fig.5 – Absolute coefficients, function db1, level 5 and wavelet image with frequency, time and amplitude for derived of North geomagnetic field.

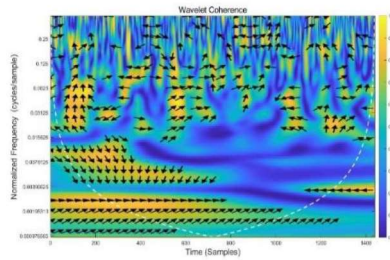


Fig.6 – Wavelet coherences between minute means of North components of the geomagnetic field, October, 28th, 2003, from Surlari Observatory and Honolulu (HON) Observatory.

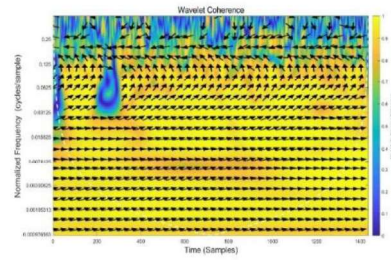


Fig.7 – Wavelet coherences between minute means of North components of the geomagnetic field, October, 28th, 2003, from Surlari Observatory and Tihany Observatory.

Section AIR POLLUTION AND CLIMATE CHANGE

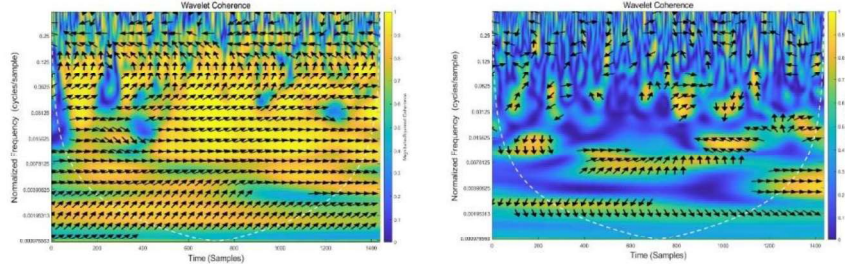


Fig.8 – Wavelet coherences between minute means of North components of the geomagnetic field, October, 28th, 2003, from Surlari Observatory and Wingst (WNG) Observatory.

Fig.9 – Wavelet coherences between minute means of North components of the geomagnetic field, October, 28th, 2003, from Surlari Observatory and Yellowknife (YKC) Observatory.

In figures 6-9 are shows the wavelet coherence between geomagnetic field recorded at different observatories during the geomagnetic storm and display the result. The sampling rate was 1 minute and obtained a time-frequency plot of the wavelet coherence, used to indicate the relative lag between coherent components [11], [13], [14]. The arrows are oriented in the direction of the phase difference between the two signals. We calculate for North component of the geomagnetic field, October, 28th, 2003, 0:24, minute means, from Surlari Observatory ARIMA(p,d,q) model, where: p is the number of autoregressive terms, d is the number of non-periodical differences needed for stationarity, and q is the number of lagged forecast errors in the prediction equation (Greene, W. H.. 1997; Box&Jenkins.1994; Hamilton, J. D. 1994)

We obtained the following results:

ARIMA(2,1,0) Model (Gaussian Distribution):

	Value	StandardError	TStatistic	PValue
Constant	0.014229	0.045031	0.31598	0.75201
AR{1}	0.38595	0.0065773	58.679	0
AR{2}	-0.060493	0.016828	-3.5948	0.00032461
Variance	2.823	0.014659	192.57	0

The estimated model is: $0.01\Delta y_{t-1} + 0.39\Delta y_{t-2} - 0.06\Delta y_{t-3} + \varepsilon_t$, where ε_t is normally distributed with standard deviation 0.01.

The signs of the estimated AR coefficients correspond to the AR coefficients on the right side of the model equation. In lag operator polynomial notation, the fitted model is

$$(1-0.39L+0.06L^2)(1-L)y_t = \varepsilon_t \quad , \text{ with the opposite sign on the AR coefficients.}$$



For calculate the difference the data before estimating,

ARIMA(2,0,0) Model (Gaussian Distribution):

	Value	StandardError	TStatistic	PValue
Constant	0.014245	0.045062	0.31611	0.75192
AR{1}	0.38595	0.0065819	58.639	0
AR{2}	-0.060494	0.016839	-3.5924	0.00032768
Variance	2.825	0.01468	192.44	0

The parameter point estimates are very similar to those in EstMdl. The standard errors, however, are larger when the data is differenced before estimation. Forecasts made using the estimated AR model (EstMdlAR) will be on the differenced scale. Forecasts made using the estimated ARIMA model (EstMdl) will be on the same scale as the original data. ARIMA includes moving average (MA), autoregressive (AR), mixed autoregressive and moving average (ARMA), integrated (ARIMA), multiplicative seasonal, and linear time series models that include a regression component (ARIMAX).

CONCLUSION

The use of multi-resolution analysis and different models for the prediction of geomagnetic disturbances, together with the energy and conductivity data of the subsoil, facilitates the calculation of GIC in a variety of situations. A simple but effective way to highlight a geomagnetic storm is calculation gradients of geomagnetic components. sudden geomagnetic variation (SSC, SI, SFE, geomagnetic storms) are relevant through Kp index (only for geomagnetic storms calculated for INTERMAGNET observatories). The Kp indexes = (5-,4,9,8,8-,8-,9-,9-) and Ap=204, from the site <https://www.spaceweatherlive.com/en/archive>, qualify the perturbations from October 28, 2003, in the category of events, as very strong storms. The statistical and spectral analysis of the geomagnetic field variation from geomagnetic observatories provides information on the geomagnetic pattern.

Fourier analysis highlights the predominant frequencies of magnetic field components. Wavelet analysis provides information about the frequency ranges of magnetic fields during the time. Also, the wavelet analysis allows us to decompose geomagnetic signals in different waves. The analyzes presented are significant for the studied of the geomagnetic storm. The data for the next days after the storm showed a mitigation of the perturbations and a transition to a quiet day of the geomagnetic field.

In both, the Fourier Transformation and the Wavelet Transformation, transformation evaluation involves the calculation of a scalar product between the analyzed signal and a set of signals that form a particular base in the vector space of the finite energy signals. Fourier representation use and orthogonal vectors base, whereas in the case of wavelet there is the possibility to use also bases consisting of independent linear non-orthogonal vectors. Unlike the Fourier transform, which depends only on a single parameter, wavelet transform type depends on two parameters, a and b. As a result, the graphical representation of the spectrum is different, wavelet analysis bringing more information about geomagnetic pattern of

Section AIR POLLUTION AND CLIMATE CHANGE

each observatory with that own specific conditions. Wavelets, can distinguish between different relationships that occur at the same time but at different frequencies. Also, is useful for all types of time-data comparisons in both the time and frequency domains, as well as in obtaining information on the different phases through which the study variables progress

ACKNOWLEDGEMENT

We gratefully acknowledge the many and significant contributions and comments provided by our colleagues from geomagnetic observatories and INTERMAGNET.

Also, we thank for support by the Ministry of Research for financing of the projects: “The realization of 3D geological / geophysical models for the characterization of some areas of economic and scientific interest in Romania”, with Contract no. 28N / 2019 and project Nr.16PCCDI/2018: „Institutional capacities and services for research, monitoring and forecasting of risks in extra-atmospheric space”, within PNCDIII.

REFERENCES

- [1] Asimopolos, N. S. and Asimopolos, L. 2018. Study on the high-intensity geomagnetic storm from march 2015, based on terrestrial and satellite data, *Micro and Nano Tehnologies & Space Tehnologies & Planetary Science, Issue 6.1, SGEM 2018*, vol.18, pp. 593-600, ISBN 978-619-7408-50-8, ISSN 1314-2704, DOI: 10.5593/sgem2018/6.1
- [2] Asimopolos, L., Niculici, E., Săndulescu, A. M. and Asimopolos, N. S. 2011. Comparisons of geomagnetic data measured in Romania with the data of International Geomagnetic Reference Field 11 (IGRF 11) - *Surveying Geology & Mining Ecology Management*, ISSN 1314-2704, DOI: 10.5593/sgem2011, vol 2, pp. 25-32
- [3] Benoit, S.L. 2012. INTERMAGNET Technical reference manual - Version 4.6, Murchison House West Mains Road Edinburgh EH9 3LA UK, pp.100.
- [4] Box, G. E. P., G. M. Jenkins, and G. C. Reinsel. 1994. *Time Series Analysis: Forecasting and Control* 3rd ed. Englewood Cliffs, NJ: Prentice Hall.
- [5] Chatfield, C. 1989. The Analysis of Time Series: An Introduction. 4th Ed. Chapman and Hall, 241 pp.
- [6] Daubechies, I. 1990. The wavelet transforms time-frequency localization and signal analysis. *IEEE Trans. Inform. Theory*, 36, pp. 961–1004.
- [7] Enders, W. 1995. *Applied Econometric Time Series*. Hoboken, NJ: John Wiley & Sons.
- [8] Gannon J. L., Swidinsky A. and Xu Z. 2019. Geomagnetically Induced Currents from the Sun to the Power Grid, *Geophysical Monograph Series*, the



American Geophysical Union, published by John Wiley & Sons, Inc., ISBN: 9781119434344

[9] Gebbins D., Herrero-Bervera,E. 2007. Encyclopedia of Geomagnetism and Paleomagnetism – Springer, pp.311-360/1072.

[10] Greene, W. H. 1997. *Econometric Analysis*. 3rd ed. Upper Saddle River, NJ: Prentice Hall.

[11] Hafner C. M. 2012. Cross-correlating wavelet coefficients with applications to high-frequency financial time series, *Journal of Applied Statistics*, vol. 39, pp. 39–36.

[12] Hamilton, J. D. 1994. *Time Series Analysis*. Princeton, NJ: Princeton University Press.

[13] MATLAB Software. 2011. The Language of Technical Computing, The MathWorks.

[14] Torrence, C., Compo, G.P. 1998. A Practical Guide to Wavelet Analysis, *Bulletin of the American Meteorological Society*, Vol. 79, No. 1, January, pp. 61-78.